# Climate change altered the dynamics of stand dominant height in forests during the past century – Analysis of 20 European tree species

Matthieu Combaud, Thomas Cordonnier, S. Dupire, Patrick Vallet

# Climate change altered the dynamics of stand dominant height in forests during the past century - analysis of 20 European tree species

**Running head:** Climate change altered forest height dynamics

**Authors and institutional affiliations:** COMBAUD Matthieu[1] (orcid : 0009-0009-8831-375X), CORDONNIER Thomas[1,2] (orcid : 0000-0003-3684-4662), DUPIRE Sylvain[1] (orcid : 0000-0001-9279-1660) VALLET Patrick[1] (orcid : 0000-0003-2649-9447)

[1] Univ. Grenoble Alpes, INRAE, LESSEM, F-38402 St-Martin-d'Hères, France

[2] Office National des Forêts, Recherche Développement et Innovation, 21 rue du Muguet 39100 Dole, France

**Contact information:** VALLET Patrick, +33 (0)4 76 76 27 34, patrick.vallet@inrae.fr

**Keywords:**

- adaptation to climate change
- climate - growth relationship
- European forest
- long term climate database
- national forest inventory

- dynamic growth equation

**Authors' contributions:** **Matthieu Combaud:** Conceptualization, Data preparation, Methodology, Modeling implementation, Validation, Analysis, Writing of the manuscript. **Thomas Cordonnier:** Conceptualization, Methodology, Validation, Analysis, Writing of the manuscript. **Sylvain Dupire:** Data preparation, Validation, Analysis, Writing of the manuscript. **Patrick Vallet:** Conceptualization, Data preparation, Methodology, Validation, Analysis, Writing of the manuscript.

**Authors' conflict of interest:** The authors declare that they have no known competing financial interests or personal relationships that could have appeared to influence the work reported in this paper.

## Abstract

Analyzing how climate change has affected forest growth is crucial for predicting future dynamics and adapting forest management to future climate change. In this paper, we investigate how climate change has modified stand dominant height dynamics and site index of 20 European tree species. We used an innovative method based on an annual height increment equation to model stand dominant height as a function of climate back to 1872 and of other stand environmental conditions. We used these models to simulate stand dominant height dynamics and site index under two different climates (prior to climate change and actual recent climate) to analyze the impact of climate change over the past

century. To build our models, we combined the recently published FYRE long-term climate database, which provides daily data since 1871, with data from more than 17,000 forest stands of the French National Forest Inventory network. Higher temperature, precipitation and climatic water balance generally favor stand dominant height dynamics when the variables are considered separately. However, the positive effects often saturate at the higher end of the variable distribution. Over the past century, the effect of climate change on the site index has varied widely among species, ranging from a decrease of less than 3% to an increase of more than 5%. The effect of climate change has also varied within species, with more positive effects on initially temperature-limited stands for some species. For the species and environmental conditions considered, our results highlight a positive response of site index to past climate change for most species, albeit with between- and within-species differences. Our results also suggest that this positive response could become negative under continued climate change. These conclusions, as well as the quantitative relationships we provide between climate and stand dominant height dynamics or site index, will help design management strategies to adapt forests to climate change.

## 1. Introduction

In the context of rapid climate change, indicators used in forest management should take into account the impact of climate change on forest dynamics. This is a prerequisite for implementing management strategies that promote adaptation to climate change.

Stand productivity, defined as “the potential of a particular forest stand to produce aboveground wood volume” (Skovsgaard and Vanclay, 2008) is a key indicator for forest

60 management (Socha et al., 2020). Since it largely depends on climatic and soil factors, it is
61 important to develop models assessing the impact of climate change on site productivity. In
62 pure even-aged stands, the average height of the tallest trees, defined as “dominant height”,
63 is an interesting indicator to analyze stand productivity. In such stands, the increase in
64 stand dominant height indeed correlates with stand volume growth and is largely
65 independent of stand density, provided that thinning is not done from above (Skovsgaard
66 and Vanclay, 2008). A common indicator of stand productivity in pure even-aged forest is
67 therefore site index, defined as stand dominant height at a given reference age, *e.g.* at 100
68 years (Skovsgaard and Vanclay, 2008).

69 Stand dominant height dynamics and site index depend on environmental conditions
70 (Vallet and Perot, 2016; Sharma et al., 2015; Scolforo et al., 2020). It is therefore important
71 to better understand how climate change affect both. Existing studies across a variety of
72 species and contexts have generally found a positive effect of higher temperature and water
73 availability on site index (*e.g.* Messaoud and Chen, 2011; Brandl et al. 2018; González-
74 Rodríguez and Diéguez-Aranda, 2021) and stand dominant height dynamics (*e.g.* Vallet and
75 Perot, 2016). However, the sign and magnitude of climate effect vary among species and
76 environmental conditions (Albert and Schmidt, 2010; Pau et al., 2022) and the positive
77 effects of temperature or precipitation may saturate when they reach a certain level (*e.g.*
78 Brandl et al., 2018). Such climate–growth relationships have been well studied for some
79 iconic European tree species such as *Picea abies* (L.) H.Karst or *Fagus sylvatica* L.. However,
80 climate–growth relationships are scarcer for other species such as *Quercus pubescens* Willd.,
81 *Fraxinus excelsior* L. or *Larix decidua* Mill., and it would be useful for forest managers to
82 have information for a larger number of species.

The site index for a given site depends on the year of establishment of the stand, in relation to changes in climate, atmospheric $CO_2$ concentration, or N deposition (Sharma et al. 2012; Socha et al., 2021; Messaoud et al., 2022). Bontemps et al. (2012) even found that environmental changes during stand lifetime influence the stand dominant height dynamics, suggesting that the site index evolves during stand lifetime. However, to our knowledge, empirical quantitative relationships on the scale of stand lifetime between on the one hand stand dominant height dynamicsor site index and on the other hand climate change are still lacking for many species. Such relationships would be very useful for forest management to anticipate short-term effects of climate change on stand productivity.

One challenge in establishing these relationships is relating stand dominant height observations to climate data at the scale of the year (or a few years). One solution would be to relate annual (or multi-year) climate data to height data at the same temporal resolution. Such high-frequency height data come mainly from stem analysis (Bontemps and Bouriaud 2014). However, stem analysis often focuses on a low number of species and comes at the cost of a small number of observations (Bontemps and Bouriaud 2014). This may limit the ability to identify a relationship between climate and stand dominant height, and this may limit the range of climate conditions to which the relationship applies. In contrast, national forest inventories (NFIs) provide large-scale, spatially intensive, randomly sampled data from forest stands and include a large number of species (Bontemps and Bouriaud, 2014; Aguirre et al., 2022). They therefore allow the detection of climate impacts under different resource limitations (Charru et al., 2017). National forest inventories have been used to infer relationships between climate and site index (Brandl et al., 2018) and between climate and stand dominant height dynamics (Vallet and Perot, 2016; Stimm et al., 2021). However,

106 these inventories generally do not include annual series of age and height measurements
107 from the year of establishment. This makes it difficult to study the effects of climate change
108 over the lifetime of stands, and generally leads to building stand dominant height models
109 based only on an aggregate equation linking mean climate to observed stand dominant
110 height (Vallet and Perot, 2016).

111 Spatial heterogeneity in climate influences the effects of climate change on stand dominant
112 height dynamics and site index for a given species or between species. For example, Albert
113 and Schmidt (2010) showed that *Picea abies* site index responded more negatively to
114 climate change in water-limited environments and *Fagus sylvatica* site index responded
115 more positively to climate change in temperature-limited environments. Generalizing such
116 results to a larger number of species could help to design forest adaptation strategies to
117 climate change.

118 This paper has three main objectives: first, to develop species-specific models linking
119 climate to stand dominant height dynamics for a large number of European tree species,
120 capable of capturing the impact of climate variation during stand life and accounting for
121 non-linear climate effects; second, to analyze the effect of each climatic variable on site
122 index; third, to assess the impact of climate change over the past century on stand dominant
123 height dynamics and site index.

124 To this end, we developed an original modeling strategy that takes into account the
125 influence of annual climate on stand dominant height dynamics even without repeated
126 measurements of stand dominant height. This strategy allowed us use the data from the
127 French National Forest Inventory (IGN, 2022) and thus to calibrate our models on more

than 17,000 stands covering a wide range of species and climate conditions. This modeling strategy relies on the reconstruction of an unobserved stand dominant height trajectory from stand origin based on initial stand dominant height, stand age, and a theory-based stand dominant height increment equation (Tomé et al., 2006; Bontemps et al., 2009) incorporating annual climate. This approach relies critically on the long-term FYRE climate database, which dates back to 1871(Devers et al., 2021). We then used these models to assess the impact of climate change during the past century by comparing simulated stand dominant height dynamics (and site index) under two scenarios: with a climate prior to climate change and with actual climate.

Based on these stand dominant height models taking into account annual climate and the associated simulations, we examined the following question:

- Question 1: How do individual climatic variables influence stand dominant height and site index? We tested the following hypotheses:
  - Hypothesis 1: Higher temperature, precipitation and climatic water balance during spring and summer favor site index, but these positive effects may saturate beyond a certain value, and in the case of temperature may even be reversed.
- Question 2: What was the effect of climate change on stand dominant height and site index during the last century? We tested the following hypotheses:
  - Hypothesis 2a: Climate change has had a different effect (sign and magnitude) depending on the species during the period considered;

- Hypothesis 2b: For a given species, the effect of climate change during the period considered varied depending on the climate context of the stand.

# 2. Materials and methods

## 2.1. General approach

For each of 20 European tree species, we built a species-specific model to relate observed stand dominant height (SDH) to (i) SDH at the stand establishment date, (ii) climate data series from the stand establishment date, and (iii) other site variables. We then used these models to simulate the SDH dynamics of each stand for a period of 70 years under a reference climate representing the climate before climate change (1891-1920 mean climate) and under the actual climate of the recent period (1950-2020 climate series). This allowed us to evaluate the impact of climate change on SDH dynamics during the last century. We then computed simulated site index as simulated SDH at the age of 70 years. Therefore, simulated site index depends on stand climate history, which enabled us to study the impact of climate change on site index.

## 2.2. Data used for modeling and simulation

### 2.2.1. National Forest Inventory data and variables

We used data from the French National Forest Inventory (IGN, 2022) from 2006 to 2020. Each year, 5000 to 6000 temporary forest plots are measured throughout the French metropolitan territory, through a progressive survey of a grid with a resolution of 1 km. This ensures uniform coverage of the territory for each measurement year. For each stand,

169 the NFI data provides canopy cover per tree species and forest vertical structure (even-
170 aged or uneven-aged forest), determined within a 25m-radius circle. Dominant trees are
171 defined as the six largest-diameter trees in a 15m-radius circle. Age and height are
172 generally measured for two of these dominant trees, referred to as "measured dominant
173 trees" in the rest of this section. In some specific configurations (a single living tree, or high-
174 value trees that could not be cored), a single dominant tree is measured. Supplementary
175 Material A give some details on these data, which are described in detail in IGN (2022) and
176 in Vallet and Perot (2016).

177 ### 2.2.2. Stands and species selection

178 We considered even-aged pure stands. We defined a stand as even-aged if (i) the NFI
179 labeled it as such, and (ii) in case two dominant trees were measured, the difference in age
180 between the oldest measured dominant tree and the youngest measured dominant tree is
181 below 25% of the age of the youngest measured dominant tree. The latter condition
182 ensured that all dominant trees in the stand share roughly the same history. We considered
183 a stand to be pure if all of the following conditions were met: (i) a single species represents
184 more than 75% of the canopy cover, (ii) both measured dominant trees belong to the same
185 species, and (iii) the species with the highest canopy cover had the highest basal area. We
186 excluded stands with incomplete data (*cf.* section 2.2.4 and 2.2.5 for the list of explanatory
187 variables) and stands whose establishment date was older than the depth of the climate
188 data, namely 1871 (*cf.* section 2.2.3. for the calculation of stand establishment date). Finally,
189 we considered the 20 species with the highest number of observations in the NFI database.
190 We ended with 17,462 stands. For 15,802 of them, age and height were measured for two

trees, and for the others, age and height were measured for a single tree. Table 1 shows the list of species studied together with the corresponding number of stands. We show the geographic repartition of the stands per species in supplementary materials (Fig. A.1).

#### 2.2.3. Calculation of stand age, stand dominant height at observation date and stand establishment date

Following Assmann and Davis (1970), we defined SDH as the average height of the 100 biggest trees within a hectare. To get SDH over an area of $n$ hundred-square-meters ($n < 100$), SDH has to be computed as the mean height of the $n-1$ biggest trees to correct for sample bias (Vallet and Perot, 2016). According to the French NFI protocol, the two measured dominant trees are selected within the six biggest trees over a 7 hundred-square-meters surface, so the mean height of these two trees provides an unbiased estimate of SDH at the observation year (Vallet and Perot, 2016). Therefore, we calculated SDH at the observation year as the mean height of the two measured dominant trees. We defined stand age as the average age of the two measured dominant trees. We defined stand establishment date as the NFI observation year minus stand age. The NFI protocol defined tree age as the number of years between the date when the tree height was 1.3 m and the observation date. Therefore, at the stand establishment date, SDH was always 1.3 m. When age and height were measured for a single tree, we considered stand age and SDH to be equal to respectively the age and height of that tree. This still provided us with an unbiased estimation of stand dominant height. Damaged trees were excluded from our calculation. If NFI stand surveys were conducted between January and April of year $t$, the stand had not yet benefited from the spring and summer growing season of that year, so we considered

213 the observation year to be $t - 1$. Table 1 shows the SDH distribution, stand age distribution

214 and stand establishment date range per species.

| | | SDH (m) | | Age (year) | | | | Stand establishment date | |
|---|---|---|---|---|---|---|---|---|---|
| Species | Number of stands | Mean | s.d | Mean | s.d. | Min | Max | Min | Max |
| *Abies alba Mill., 1768* | 817 | 25.5 | 6.2 | 72.7 | 33.6 | 9 | 147 | 1871 | 2002 |
| *Betula pendula Roth, 1788* | 106 | 16.0 | 4.5 | 31.2 | 16.5 | 4 | 83 | 1932 | 2009 |
| *Carpinus betulus L., 1753* | 97 | 19.5 | 4.9 | 63.4 | 25.5 | 11 | 125 | 1885 | 2003 |
| *Castanea sativa Mill., 1768* | 440 | 17.7 | 4.8 | 43.9 | 26.1 | 5 | 141 | 1871 | 2013 |
| *Fagus sylvatica L., 1753* | 1,470 | 23.4 | 7.2 | 83.1 | 35.0 | 8 | 147 | 1871 | 2006 |
| *Fraxinus excelsior L., 1753* | 334 | 21.6 | 6.9 | 50.9 | 28.2 | 6 | 131 | 1875 | 2011 |
| *Larix decidua Mill., 1768* | 151 | 19.0 | 6.1 | 67.5 | 36.0 | 7 | 137 | 1873 | 2009 |
| *Picea abies (L.) H.Karst., 1881* | 1,338 | 22.9 | 6.6 | 42.7 | 22.5 | 7 | 145 | 1871 | 2011 |
| *Picea sitchensis (Bong.) Carrière, 1855* | 143 | 22.3 | 6.9 | 31.0 | 10.3 | 5 | 63 | 1944 | 2013 |
| *Pinus halepensis Mill., 1768* | 344 | 12.5 | 3.9 | 50.1 | 23.6 | 6 | 137 | 1875 | 2010 |
| *Pinus nigra subsp. nigra J.F.Arnold, 1785* | 413 | 15.0 | 5.3 | 53.2 | 29.3 | 6 | 135 | 1881 | 2012 |
| *Pinus nigra var. corsicana (Loudon) Hyl., 1913* | 526 | 16.0 | 5.9 | 30.6 | 20.3 | 4 | 146 | 1871 | 2015 |
| *Pinus pinaster Aiton, 1789* | 2,424 | 16.8 | 6.5 | 30.3 | 20.8 | 2 | 132 | 1876 | 2018 |
| *Pinus sylvestris L., 1753* | 1,551 | 15.8 | 5.9 | 59.3 | 27.6 | 5 | 144 | 1873 | 2011 |
| *Pseudotsuga menziesii (Mirb.) Franco, 1950* | 1,449 | 24.1 | 8.6 | 30.6 | 13.0 | 4 | 110 | 1910 | 2015 |
| *Quercus petraea (Matt.) Liebl., 1784* | 2,472 | 22.2 | 6.1 | 80.6 | 33.4 | 7 | 149 | 1871 | 2010 |
| *Quercus pubescens Willd., 1805* | 1,019 | 13.9 | 4.3 | 67.6 | 25.0 | 7 | 145 | 1871 | 2006 |
| *Quercus robur L., 1753* | 2,105 | 20.7 | 5.4 | 70.3 | 30.9 | 8 | 149 | 1871 | 2006 |
| *Quercus rubra L., 1753* | 114 | 18.5 | 6.2 | 26.4 | 16.3 | 4 | 81 | 1930 | 2006 |
| *Robinia pseudoacacia L., 1753* | 149 | 18.0 | 5.1 | 32.3 | 18.0 | 5 | 94 | 1916 | 2014 |

*Table 1: Calibration data. Only stands with complete data and with establishment date from 1871 are considered.*

*NFI data contain a single SDH measure for each stand. s.d. : standard deviation*

### 2.2.4. Climate data and climate variables

We used temperature and precipitation data from the FYRE database (Devers et al., 2020a; 2020b; 2021) for the period 1871-2012 and the Météo France SAFRAN database (Vidal et

al., 2010) for 2013-2020. This temporal depth was necessary to cover the full stand life span observed in our data. The Safran data consist in an interpolation merging observations and background data over 608 climatologically homogeneous zones covering metropolitan France, then disaggregated onto a 8 km grid taking into account altitude (Devers et al., 2020). FYRE data consist in a reanalysis over the same 8 km grid, assimilating observation into the SCOPE background (Devers et al., 2020). The FYRE data include 25 climate series, which represent equally plausible meteorological series (Caillouet et al., 2019). We used the average of these 25 climate series. For both the FYRE and SAFRAN data, we converted daily data to monthly data by averaging daily temperature and summing daily precipitation. For each grid cell, we computed the mean difference between FYRE data and SAFRAN data over the period 1990-2012, and we added this difference to SAFRAN data over 2013-2020 to correct for the bias between the two data sources. We used the 1990-2012 period to compute the bias because it represents a compromise between having enough data and covering a period close enough to the period over which we want to implement the correction (namely 2013-2020). We then created a single gridded climate database by concatenating FYRE data over 1871-2012 and SAFRAN unbiased data over 2013-2020.

To derive the temperature series at each NFI site, we corrected the grid-based climate data for an elevation gradient following Devers et al. (2020). For each of the 608 homogeneous climate areas, we defined an altitude gradient by fitting a linear model between the mean temperature and the mean altitude of each grid cell. In case there was less than three grid cells in a homogeneous climatic area, we grouped these cells with the cells of the closest homogeneous climatic area. We used this gradient to correct the climate series for each NFI site, based on the difference between the NFI site elevation and the corresponding grid cell

243 elevation. We applied a similar procedure to determine precipitation at each NFI site.
244 Because elevation correction for precipitation is not relevant in lowland areas, we applied
245 the correction only when the difference between the NFI site elevation and the
246 corresponding grid cell elevation was greater than 300m (Devers et al., 2020)

247 To combine the influence of temperature and precipitation, we calculated a monthly
248 climatic water balance, defined as the difference between precipitation and potential
249 evapotranspiration (Lebourgeois and Piedallu, 2005). Potential evapotranspiration was
250 derived from monthly temperature and radiation using the Turc formula (Lebourgeois and
251 Piedallu, 2005). Monthly radiation without nebulosity was obtained following Piedallu and
252 Gégout (2007). Since this radiation varies little between years, we assumed that the
253 monthly radiation was equal to the monthly values for the year 2000. To account for light
254 interception by clouds, we corrected the radiation value with the average monthly
255 nebulosity between 1960 and 2019, following Piedallu and Gégout (2007). The nebulosity
256 data were taken from Harris et al. (2020).

257 We defined climate year $t$ as the period from September of year $t-1$ to August of year $t$.
258 We did this because growth during the growing season of year $t$ can be influenced by
259 precipitation during the previous fall and winter (Bravo-Oviedo et al., 2008). This definition
260 led us to limit our analysis to the climate years 1872-2020, since the FYRE database starts
261 in January 1871.

262 For each stand and each climate year $t$, we calculated mean temperature, total precipitation,
263 and total climatic water balance for fall (September to November of year $t-1$), winter
264 (December of year $t-1$ to February of year $t$), spring (March to May of year $t$) and summer

(June to August of year $t$) as well as for two semesters (September of year $t-1$ to February of year $t$ and March of year $t$ to August of year $t$) and for the entire climate year. We calculated the annual sum of growing degree days (SGDD), defined as the sum of temperature above 5.5°C over all days from January to December (Kunstler et al., 2021). In this calculation, we approximated daily temperature based on the mean temperature of the corresponding month. In total, we retained 22 climatic variables.

We defined a reference climate to represent the climate prior to climate change. For each climatic variable, we defined the reference climate as the mean of the variable over the period 1891-1920. Figure 1 shows the distribution of annual climatic variables per species for the reference climate and climate anomalies over the recent period (1950-2020) compared to the reference climate.

To calibrate our models, we standardized each of the 22 climatic variables per species by subtracting the mean and dividing by the standard deviation. For each species, we calculated the mean and standard deviation based on the distribution of each variable across all stands of that species for the period 1872-2020.

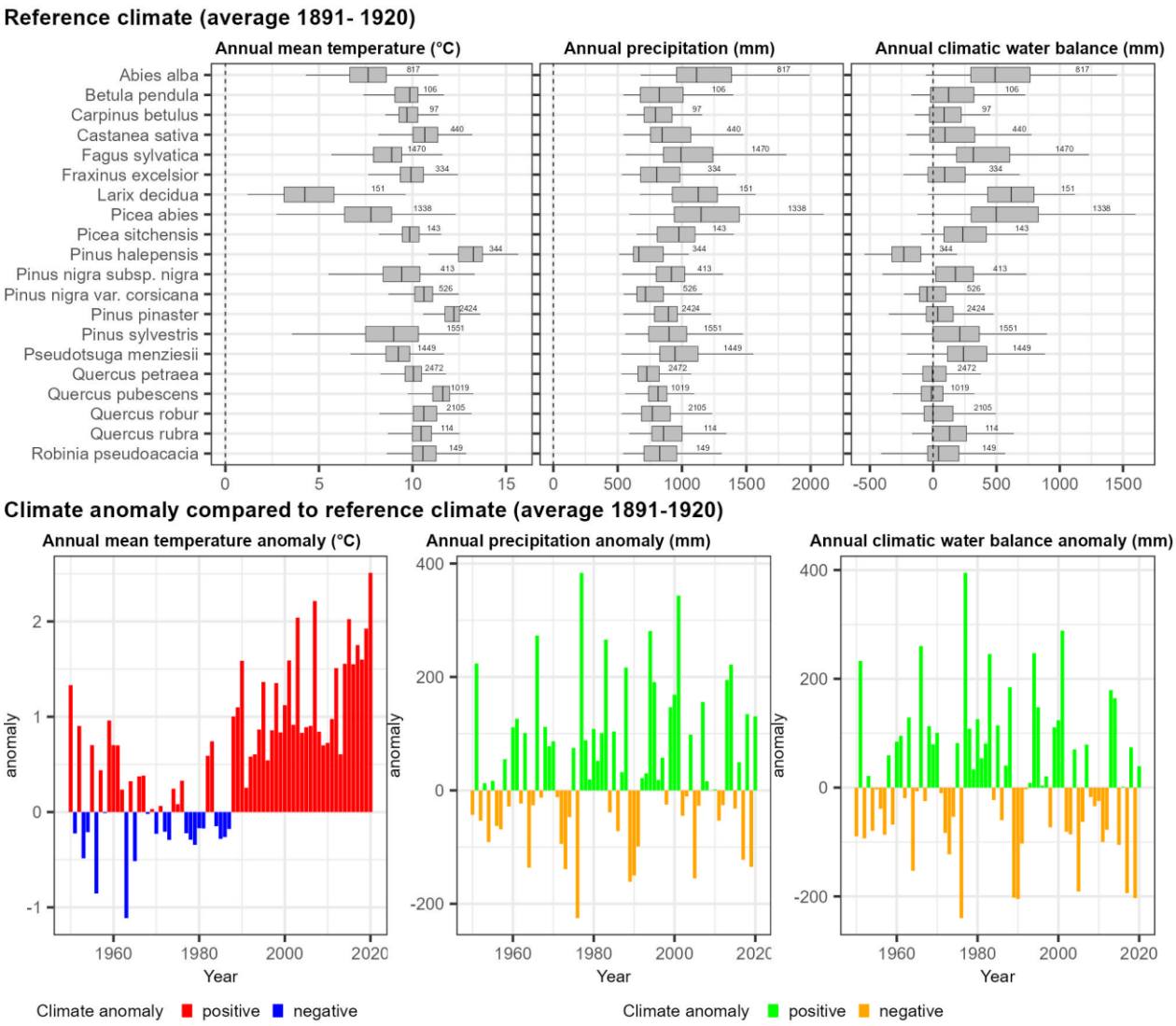


280

281 *Figure 1: Reference climate per species (first row) and climate anomalies in the recent period*

282 *(1950-2020) compared to the average of the reference period (1891-1920) (second row), for*

283 *mean temperature (left), total precipitation (middle) and total climatic water balance (right).*

284 *A higher climatic water balance corresponds to a wetter climate. In the second row, the result*

285 *for a given year is obtained by averaging all stands, regardless of species.*

### 2.2.5. Non-climate environmental data s

The French NFI provides field data for soil texture, soil depth, rock presence, rock emergence, slope and herbaceous species presence. We used NFI data on herbaceous species presence to calculate bioindicated values for C:N ratio, $P_2O_5$ and soil pH (Gégout et al., 2005). We calculated a soil water holding capacity following Piedallu et al. (2018) based on NFI data on soil texture, soil depth, and rock presence and emergence. This calculation was not possible for soils labeled as "organic soil" in NFI data, so we excluded such stands from the analysis (21 stands). Finally, NFI data do not provide field measurement of slope for stands located on complex topography. Therefore, we excluded such stands from the analysis (288 stands). Supplementary Material C provides details and summary statistics for the 14 non-climatic variables (Tab. C.1 to C.4). To calibrate our models, we standardized each of the non-climate environmental variables per species by subtracting the mean and dividing by the standard deviation. For each species, we calculated the mean and standard deviation based on the distribution of each variable across all stands of that species.

## 2.3. Modeling stand dominant height and site index as a function of annual climatic variables

### 2.3.1. Model equations

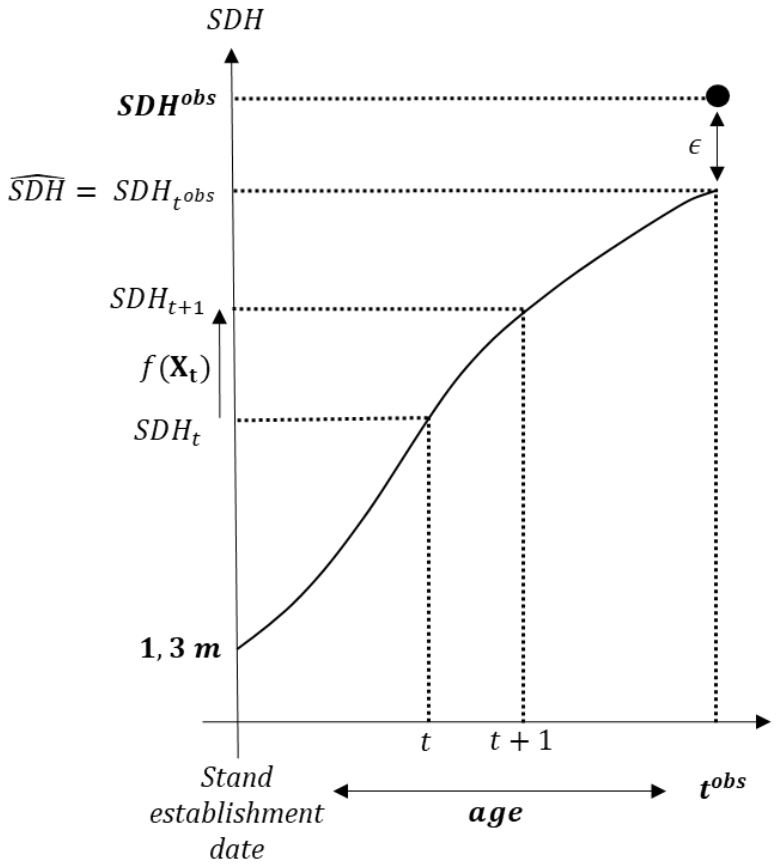


*Figure 2: Modeling strategy to model stand dominant height (SDH) dynamics of a given stand. Variables available in the NFI database or climate database are shown in bold: observed SDH ($SDH^{obs}$), stand observation year ($t^{obs}$), stand age (age) and annual environmental conditions ($X_t$). $\widehat{SDH}$ is the modeled SDH at the time of observation and $\epsilon$ is the modeling error. From the stand establishment date ($t^{obs} - age$), we reconstructed the unobserved annual trajectory of SDH ($SDH_t$) year by year using a theory-based function (f) that relates*

*the unobserved SDH increment between year t and t+1 to observed contemporary environmental conditions.*

The French NFI data do not include observations for annual SDH or SDH annual increment, so it was not possible to model directly SDH increments as a function of annual climate. We therefore used an indirect strategy (cf. Figure 2): for each species, we modeled SDH observations (one per stand) as a function of the series of annual climatic stand conditions from stand establishment date and of non-climatic stand conditions. Our model relies on the fact that (i) SDH at a given age is the sum of annual SDH increments over the period between stand establishment date and the age considered and (ii) annual SDH increments can be described by a theoretical function of non-climatic conditions, climatic conditions and SDH at the beginning of the period (Bontemps et al., 2009; Zeide, 1993).

Equation 1 describes for a given stand the relationship between observed stand dominant $SDH^{obs}$ and the series of SDH increment ($\Delta SDH_t$). In this equation, 1.3 meters is the stand dominant height at the stand establishment date (*cf.* section 2.2.3), $t^{obs}$ is the observation year, $age$ is the age, and $\epsilon$ is a heteroscedastic Gaussian residual error. To take into account increasing error with SDH, we assumed $\epsilon \sim N\left(0, \sigma^2 \widehat{SDH}^{2\delta}\right)$ where $\widehat{SDH}$ is the fitted value of SDH at the observation year for the stand under consideration, $\sigma$ is a positive parameter independent of the stand and $\delta$ is a scalar parameter independent of the stand.

$$\mathrm{SDH}^{\mathrm{obs}} = 1.3 + \sum_{\mathrm{t}=\mathrm{t}^{\mathrm{obs}}-\mathrm{age}}^{\mathrm{t}^{\mathrm{obs}}-1} \Delta\,\mathrm{SDH}_{\mathrm{t}} + \epsilon \quad \text{(Equation 1)}$$

Equation 2 describes for a given stand how we replaced unobserved annual SDH increment ($\Delta SDH_t$) by a theoretical function of environmental variables and SDH at the beginning of

the period. Zeide (1993) suggests writing SDH increment as the sum of an expansion term $f_{exp}$ and a decline term $f_{decl}$, to reflect catabolic and anabolic processes, respectively. Among the equations presented by Zeide (1993), we chose the Chapman-Richards equation because it reflects physiological processes, assuming that catabolic processes depend on size, modified by a species-specific shape term $\beta_0$, and that anabolic processes are size-dependent (Tomé et al., 2006). To ensure the biological soundness of our models, we imposed $\Delta SDH_t > 0$ to ensure that SDH does not decrease over time, for a given stand. In Equation 2, $X_t^{exp}$ and $X_t^{decl}$ are the sets of explanatory variables at year $t$ used to predict the expansion and the decline terms, respectively.

$$\Delta SDH_t = max\left[0, f_{exp}\left(X_t^{exp}\right).{SDH_t}^{\beta_0} - f_{decl}\left(X_t^{decl}\right).SDH_t\right] \quad (Equation\ 2)$$

We assumed that the expansion term was a species-specific function of the climate of the year in which the increment occurred and of other environmental variables. We assumed that the decline term was a species-specific function that depended only on temperature variables. We made this choice because the decline term reflects respiration, and respiration is primarily temperature dependent (Valentine, 1997). Finally, we assumed the shape term $\beta_0$ to be a species-specific constant. We made $f_{exp}$ and $f_{decl}$ non-divergent following Antón-Fernández et al. (2016): we expressed both $f_{exp}$ and $f_{decl}$ as a species-specific intercept ($A_0$ and $C_0$, respectively), multiplied by a logistic function of the explanatory variables (*cf.* Equation 3 and Equation 4). $\alpha$ and $\gamma$ are species-specific parameter vectors associated with the explanatory variables. We expect $A_0$ and $C_0$ to be positive, but we did not constraint the model to ease convergence. *A posterior*, we checked that the parameter value was positive or that the parameter value was not significantly

different from 0, using a p-value of 0.05 to define significance. In case there are no explanatory variable for the expansion term (resp. the decline term), the logistic function in equations 3 and 4 is replaced by a factor 0.5. This allows interpreting $\frac{A_0}{2}$ (resp. $\frac{C_0}{2}$) as the value of the expansion term (resp. decline term) for a stand at the species mean environmental conditions.

$$f_{exp}\left(X_t^{exp}\right) = A_0.\frac{exp(\alpha.X_t^{exp})}{1+exp(\alpha.X_t^{exp})} \quad (Equation\ 3)$$

$$f_{decline}\left(X_t^{decl}\right) = C_0.\frac{exp(\gamma.X_t^{decl})}{1+exp(\gamma.X_t^{decl})} \quad (Equation\ 4)$$

Equation 5 gives the final model for a given species and a given stand.

$$SDH^{obs} = 1.3 + \sum_{t=t^{obs}-age}^{t^{obs}-1} max\left[0, A_0.\frac{exp(\alpha.X_t^{exp})}{1+exp(\alpha.X_t^{exp})}SDH_t{}^{\beta_0} - C_0.\frac{exp(\gamma.X_t^{decl})}{1+exp(\gamma.X_t^{decl})}SDH_t\right] + \epsilon \quad (Equation\ 5)$$

### 2.3.2. Parameter inference and model selection

For each species, we calibrated the model presented in Equation 5 using the data presented in section 2.2. For a given set of explanatory variables, we used the *nlminb* function in the "stats" R-package version 4.2.0 (R Core Team, 2022) and the TMB R-package version 1.9.0 (Kristensen et al. 2016) to minimize the model negative log-likelihood (*nll*, given by Equation 6) with respect to the species-specific parameters $A_0, C_0, \alpha, \gamma, \beta_0$. In Equation 6, $n$ is the number of stands for the species considered, $i$ is a stand index and $\widehat{SDH_i}$ is the prediction for stand $i$ of the model given in Equation 5. The nlminb function allows optimizing expressions without simple analytical form, and the TMB package makes the computation faster.

$$nll = \frac{n}{2}.ln(2\pi) + \sum_{i=1}^{n} ln\left(\sigma\widehat{SDH}_i^{\delta}\right) + \frac{1}{2}\sum_{i=1}^{n}\left(\frac{SDH_i^{obs} - \widehat{SDH}_i}{\sigma\widehat{SDH}_i^{\delta}}\right)^2 \quad \textit{(Equation 6)}$$

For each species, we followed a stepwise variable selection process (Vallet and Perot, 2016; Mina et al., 2018). In this process, we considered the standardized 22 climatic variables and 14 non-climatic variables. We also considered the square of each climatic variable and the square of pH, C:N ratio and $P_2O_5$ indicator to identify potential saturation or non-monotonic effects. At each step, (i) for each variable non-included in the model yet, we tested the inclusion of the variable in the expansion term, (ii) for temperature variables, we also tested the inclusion in the decline term and (iii) we selected the model that most decreased the Bayesian information criterion (BIC). The BIC penalizes the inclusion of an additional variable in the model more than AIC, which limits the risk of overfitting. We repeated this process until the BIC reached its minimum. To avoid collinearity, we used a variance inflation factor (VIF) (O'Brien, 2007). We excluded all models with variables with a VIF greater than 2 from the model selection process. To avoid issues in parameter identification due to the appearance of the same variable in both the expansion and decline terms, we allowed a given temperature variable to appear either in the expansion or decline terms, but not both. For *Castanea sativa*, *Picea sitchensis*, *Quercus rubra* and *Betula pendula*, we excluded the qualitative variable reflecting the calcareous nature of the bedrock, because more than 90% of the stands were on the same type of bedrock.

### 2.3.3. Assessment of model quality

To assess the risk of overfitting for each species-specific model, we calculated the difference between model prediction error using data not used for calibration and model prediction error using calibration data. We refer to this difference in prediction error as "model

optimism". To do this, we implemented a fivefold cross-validation. First, we randomly divided our sample into five equally sized subsamples. Then we repeated the following procedure for each subsample: (i) we considered this subsample as a validation subsample and the remaining four subsamples as a single calibration subsample, (ii) we calibrated the model presented in equation 5 on this calibration subsample and (iii) we calculated the root mean square error (RMSE) over this calibration subsample and the RMSE over the validation subsample and (iv) we defined an intermediate optimism indicator as the relative difference between the RMSE calculated on the validation subsample and the RMSE calculated on the calibration subsample. If the difference was negative, we considered it to zero. We defined the final optimism indicator as the average of the five intermediate optimism indicators. The higher the optimism indicator, the higher the prediction error when the model was applied to new data compared to the error when it was applied to calibration data. Details can be found in Supplementary Material D. We also calculated the RMSE, root mean square percentage error (RMSPE) and bias of each species-specific model when calibration was done on the whole sample (*cf.* Supplementary Material D for calculation details).

### 2.4. Simulations to analyze the partial effect of climatic variables and the effect of climate change on stand dominant height and site index

To analyze the impact of each climatic variable and climate change on SDH and site index, we ran simulations based on the models we calibrated. To allow for interspecific comparisons, we stopped the simulation at age 70 years, which corresponds to the lowest

observed maximum age amongst our species (see Tab. 1). We therefore defined the site index as SDH at age 70 years.

For each species, we analyzed the partial effect of each variable, defined as the effect of a variation in that variable on site index, holding all other variables constant. To do this, we simulated the site index using the model developed in 2.3, while varying the variable from the 0.05 to the 0.95 percentile of its species-specific range. We defined this species-specific range as the distribution of annual values of the variable from 1872 to 2020 over all stands of the species. For these simulations, we set all other variables to their mean values.

We then analyzed the impact of climate change over the last century, taking into account the simultaneous evolution of the different climatic variables. For each species, we simulated the SDH dynamics of each observed stand under the pre-climate change reference climate (1891-1920 mean) and under the actual climate of the recent period (1950 to 2020 climate series). We analyzed the impact of climate change on both (i) the shape of the SDH trajectory and (ii) the percentage variation of the site index between the recent and the reference climates.

# 3. Results

## 3.1. Importance of climatic variables

Some climatic variables were selected in our models for all species except *Pinus nigra subsp. nigra* and *Picea sitchensis*. Species differed in the type of variable selected (temperature, precipitation, climatic water balance, SGDD) and the season of the year for which the variable was selected. Non-climate environmental characteristics such as C:N ratio, soil pH,

436 slope were often selected in the models. Detailed parameters are given in Supplementary
437 Material G (Table G. 1).

## 438 3.2. Performance of the models

439 Depending on the species, the RMSE varied between 2.4 m and 3.8 m and the RMSPE varied
440 between 14.3% and 29.9% over the stands used for calibration, while bias was null for all
441 species (*cf.* Supplementary Material, table D.1). Model optimism decreased with increasing
442 number of calibration points and was below 10% for all species with more than 200
443 calibration stands (*cf.* Supplementary Material Fig. D.1).

## 444 3.3. Partial effect of climatic variables on site index

445 Higher temperature, precipitation, and climatic water balance during spring and summer
446 generally favored the site index, defined as SDH at 70 years (Figure 3). For a large number
447 of species and variables, site index reached a maximum value and then saturated at the
448 upper end of the variable range. The decrease in site index at the upper end of the variable
449 distribution for some species and variables is quite weak. We also found a positive
450 saturation effect of fall and winter temperature for three species. We found more
451 contrasting results for fall and winter precipitation and climatic water balance, with a
452 positive saturating effect for some species, optimal values for other species, and a negative
453 effect for other species. The magnitude of the partial effect depended on the species and the
454 variable. Spring and summer temperature and precipitation generally had the most positive
455 effects. Our results show an outlier behavior for *Castanea sativa*: for this species, summer
456 temperature had a negative effect on the site index.

*Figure 3: Partial effect of climatic variables on site index. Each graph represents site index (y-axis) as a function of climate (x-axis). Each color represents a species. Each column corresponds to a specific season, each line corresponds to variable. First line: temperature (mean temperature of the period for the six first columns, and annual sum of growing degree days for the seventh*

*column), second line: precipitations, third line: climatic water balance. In each graph, only the species for which a climate effect was found are represented. See the Material and Methods section for an explanation of how partial effect was calculated.*

## 3.4. Effect of climate change on stand dominant height over the past century

### 3.4.1. Effect of climate change on stand dominant height dynamics

We simulated SDH dynamics for each species under both the actual 1950-2020 climate and the reference 1891-1920 average climate. To illustrate,

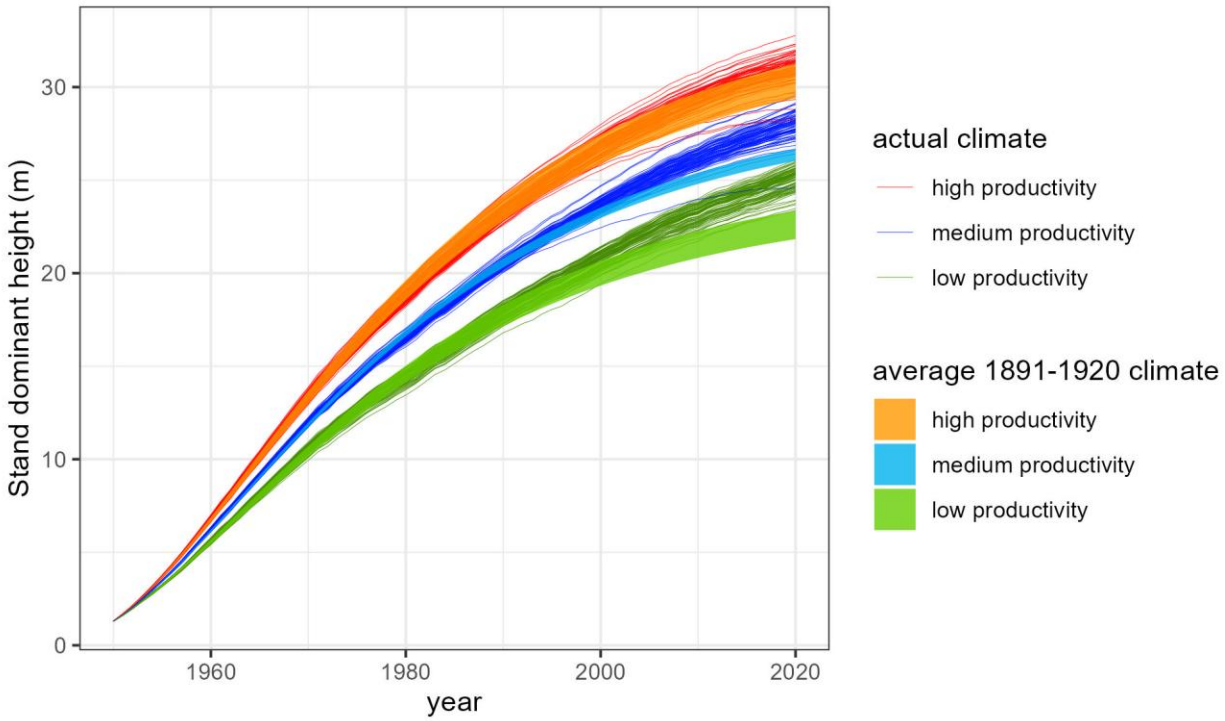


Figure 4 compares the SDH dynamics for *Abies alba*. After 40 years of almost no effect, the effect of climate change became positive. This positive effect was more pronounced at the lowest levels of productivity, where productivity is defined as the site index under the reference climate. We found a similar pattern for *Fagus sylvatica* and *Picea abies* (Supplementary Material Fig. E.1), but other species showed contrasting responses.

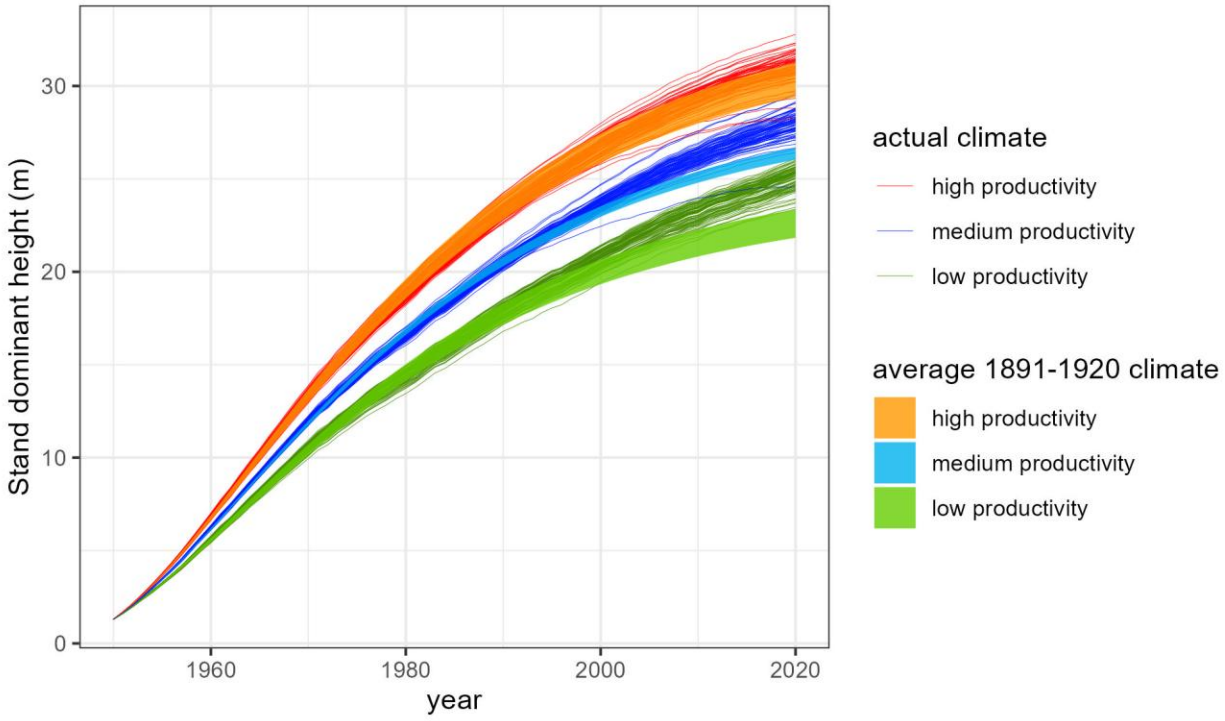


*Figure 4: Simulated SDH dynamics for actual recent climate (solid line, climate series 1950 to 2020) and reference climate (ribbon, average climate 1891-1920) for Abies alba stands. Stands were grouped into three categories according to their productivity, defined as site index under the reference climate: productivity quantiles 0.05 to 0.15 (green), 0.45 to 0.55 (blue) and 0.85 to 0.95 (red).*

### 3.4.2. Interspecific responses to climate change

The median impact of climate change on the site index was positive for 15 species, negative for three species, and null for two species (Figure 5). The positive impacts were generally stronger than the negative impacts: the median impact was above 3% for four species, while only *Castanea sativa* had a negative impact below 3%. We did not find a general interspecific pattern linking the mean climate impact to the species' climate niche prior to climate change (*cf.* Supplementary Material F, Fig. F.1 and Fig F.2).

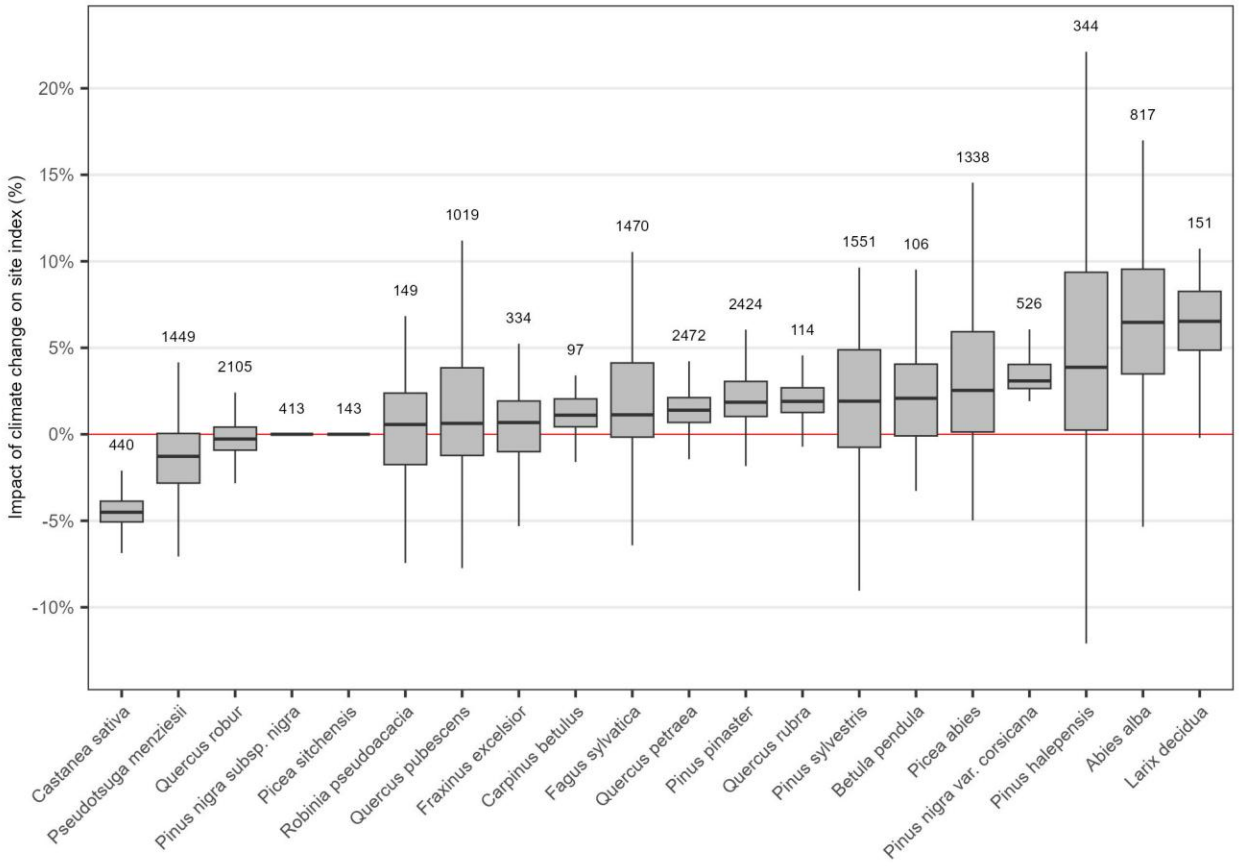


Figure 5: Climate change effect on site index. Boxplots show the distribution of climate change effect over NFI stands for each species. Climate change effect was calculated as the relative difference between the simulated site index under the actual recent climate (1950-2020 climate series) and the reference climate (1891-1920 average). For each species, the number of calibration stands is given above the box. Outliers are not shown. Intraspecific response to climate change

We found intraspecific variation in the effects of climate change on the site index (Figure 5). For six species, the median impact was positive, but the first quartile impact was negative. For nine species, the effect of climate change on the site index was positive at the cold edge of the species' temperature range and negative or close to zero at the warm edge (Figure 6).

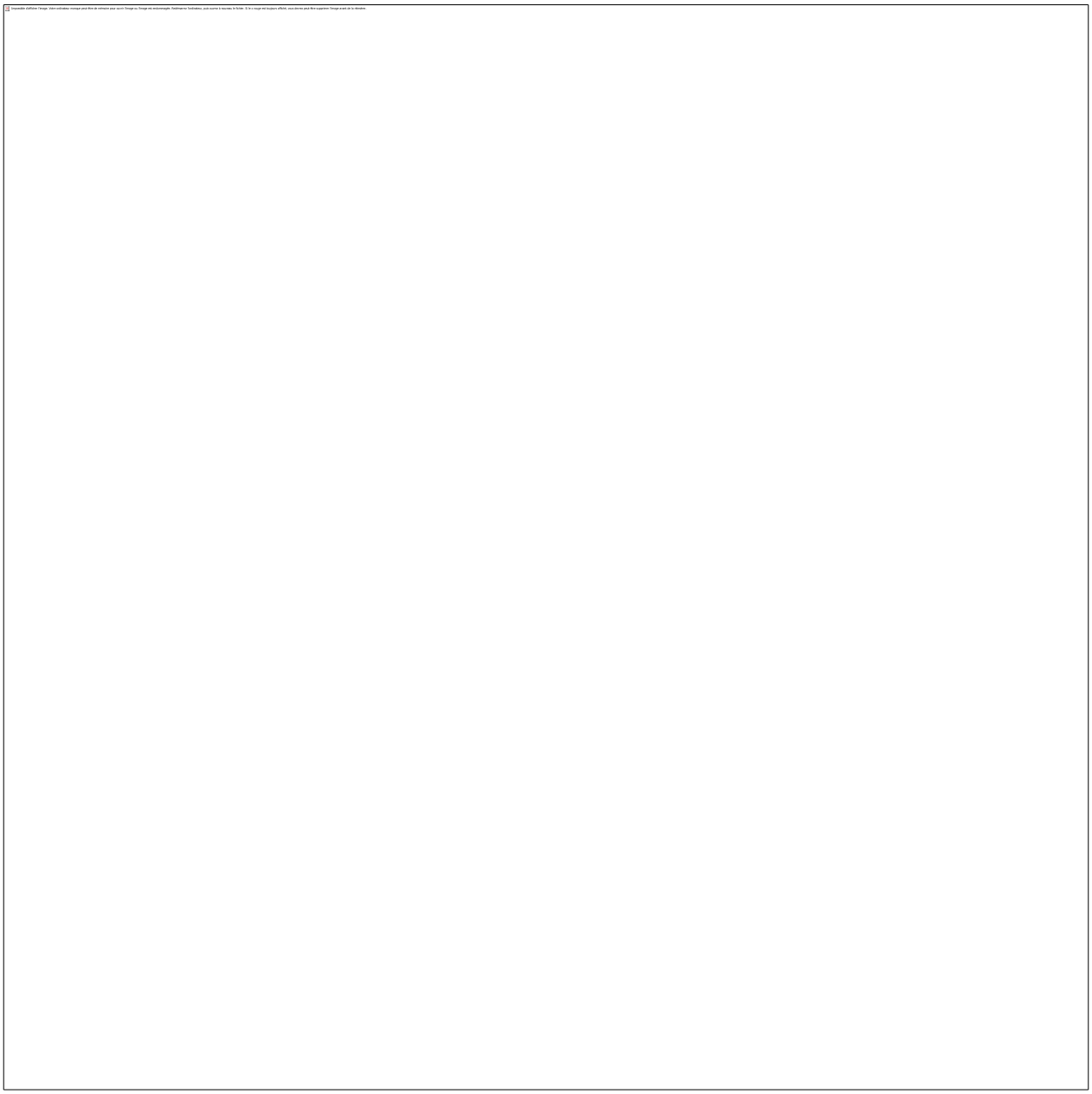

*Figure 6: Climate change effect on site index as a function of mean annual temperature over the reference period (1891-1920). Boxplots show the distribution of climate change effect on site index across the NFI stands for each species. The effect of climate change was calculated as the relative difference between the simulated site index under the actual climate (1950-2020 climate series) and the reference climate (1891-1920 average). The x-axis represents the average climate of the stand over the reference period (1891-1920). For Betula pendula, Fagus sylvatica and Pinus halepensis, some whiskers extend beyond the box; their values are*

*given at the extremities of the corresponding boxplots. Outliers are not shown. Boxplots in white are based on fewer than 10 stands.*

# 4. Discussion

In this paper, we analyzed the impact of past climate change on SDH dynamics and site index for 20 common European tree species and we analyzed interspecific and intraspecific differences in SDH and site index response to climate change. In the discussion, we first point out the interest of our modeling approach; we will emphasize some limitations of this approach; then we comment on the partial effect of climatic variable on site index; then we discuss the impact of climate change during the last century on SDH dynamics and site index, and finally we elaborate on implications for management.

## 4.1. Interest of the approach

To our knowledge, this is the first time annual SDH trajectories have been empirically modeled for 20 species, taking into account annual climate over the past century. We achieved this by combining French NFI data and FYRE long-term climate data, and by using a theory-based annual SDH increment equation. The FYRE data allowed us to model SDH dynamics for stands as old as 150 years while accounting for annual climate. The French NFI data include a large number of stands per species and cover a large climatic gradient, which allowed us to identify climate effects. Different stand age classes at the time of stand observation allowed us to partially decorrelate age with date. The French NFI data provided us with field measurements of non-climatic variables to use as covariates, limiting potential bias due to overrepresentation of older stands on infertile sites (Socha et al., 2021). The

theory-based SDH increment equation we used ensured that our approach was biologically consistent (Tomé et al., 2006).

Our approach has operational advantages over stem analysis. Stem analysis requires intensive field sampling for each stand, and is generally conducted in the context of a specific study. The number of stands used in stem analysis studies can therefore be quite limited (Bontemps and Bouriaud, 2014) although some studies are based on a large number of stands (Socha et al., 2021; Pau et al., 2022). In contrast, the French NFI data are representative of the species' distribution in the study area. They cover a large climatic gradient and include numerous stands of common species. Our approach allowed us to derive SDH-dynamics models for rarely studied species such as *Larix decidua*, *Quercus pubescens* and *Fraxinus excelsior*. The main advantage of stem analysis over our approach is that it provides a temporal series of SDH measurements, whereas our approach relies on a single SDH measurement. Stem analysis also provides more accurate height measurements compared to NFI data. In the future, it would be interesting to compare our simulated SDH dynamics with observed SDH dynamics and with SDH dynamics simulated by a model based on stem analysis.

The RMSE we found are in the same order of magnitude as in other studies based on NFI data (Seynave et al., 2008; Sharma et al., 2012) but higher than in studies based on stem analysis (Socha et al., 2021). The optimism of our models is generally low, indicating good robustness, especially for species with a large number of calibration stands. Parameter values for species with high model optimism should be used with caution.

## 4.2. Limits of the approach

The NFI data do not provide information on stand history. This forced us to make several assumptions. First, we assumed that the dominant trees at observation time had been dominant throughout stand development. This is a common assumption in SDH studies. Second, we assumed that SDH dynamics were independent of competition history. This is justified for a wide range of densities (Skovsgaard and Vanclay, 2008). The inclusion of a competition variable could still be interesting (Vallet and Perot, 2016). Third, we did not include interactions in our models because this could have led to overparameterized models. Fourth, we did not include nitrogen deposition in our model because due to a lack of historical data. This variable has been identified as an important driver of SDH in the late 20$^{th}$ century (Bontemps et al., 2011). As a proxy, we included the C:N ratio at the observation date in our models. This allowed us to account for spatial heterogeneity, but not temporal changes. Atmospheric $CO_2$ concentrations are sometimes considered to be an important driver of the increase in tree growth during the last century, but this role is still under debate, especially since the positive effect may be restricted to young stages (Asshoff, Zotz, and Körner, 2006; Boisvenue and Running, 2006; McDowell et al., 2020). We did not include this variable in our models because it would have created a temporal trend that could have prevented us from identifying the effect of climatic variables. Because we did not properly disentangle the effects of climate, atmospheric nitrogen deposition, and atmospheric $CO_2$ concentration in our models, some of the effect we attributed to climate could be related to the other two factors. Complementing this study with process-based models may be useful to disentangle these effects.

### 4.3. Partial effect of climatic variables on site index

Our results regarding the partial effect of climatic variables confirm our hypothesis 1 that an increase in temperature, precipitation and climatic water balance during spring and summer favors the site index, but that these positive effects may saturate when the climatic variable reaches a certain level. However, contrary to our hypothesis, our results do not clearly show a negative effect of temperature above a certain threshold. Indeed, the decrease of site index at the upper range of the variable distribution for some species and variables is not very pronounced and may simply reflect the fact that we integrated saturation and non-monotonic effects in the model using a quadratic form.

For commonly studied species, our results are largely consistent with the literature, especially (i) the generally positive effect of temperature and SGDD (Albert and Schmidt, 2010; Álvarez-Álvarez et al. ,2011; González-Rodríguez and Diéguez-Aranda, 2020), (ii) the generally positive effect of precipitation and climatic water balance (Vallet and Perot, 2016; Stimm et al., 2021), (iii) the saturation effect beyond a certain level of temperature (Seynave et al. 2008; Caicoya and Pretzsch, 2021; Pau et al., 2022) or precipitation (Brandl et al., 2018) and (iv) the existence of interspecific differences in the climatic variables and seasons affecting SDH (Vallet and Perot, 2016). Table 2 compares the species-specific effects we found with those reported in the literature for the five most common European tree species, as listed by (Mahnken et al., 2022). The present work allows to extend such results to species for which, to our knowledge, the climate – SDH relationship has hardly been studied yet, such as *Larix decidua*, *Fraxinus excelsior* or *Quercus pubescens*.

These effects on site index are consistent with the expected response based on tree physiology. The positive effects of higher spring and summer temperature probably relate

to an increase photosynthetic efficiency or a lengthening of the growing season (Brandl et al., 2018). Saturation may occur because temperature is no longer the limiting factor, or because high temperature increase evapotranspiration and hydric stress, and reduce photosynthesis (Lindner et al., 2010; Anderson-Teixeira et al., 2022). The lack of a clear signal of negative effects of temperature above a certain level may relate to the fact that such extreme temperature have only occurred in recent years, and therefore their effects are not well captured in our multi-decadal modeling strategy. The negative effect of high winter temperature for some species may relate to disturbance of bud break or high winter respiration (Seynave et al., 2008). The generally positive impact of spring and summer precipitation and climatic water balance, and the saturation of this positive effect at the wetter edge of the range, may be related to a positive effect of relaxing the water constraint only in water-limited environments. With respect to fall and winter precipitation and climatic water balance, the interspecific diversity of responses suggests that species have different levels of tolerance to water excess or develop under specific stand conditions. Negative responses can be explained by nutrient depletion in the case of too much water (Álvarez-Álvarez et al., 2011) or by snow damage (Seynave et al., 2008). The outlier behavior of *Castanea sativa* (negative effect of summer temperature) could be due to the impact of the chestnut ink disease, which can hinder tree growth, especially under drought conditions (Maurel et al., 2001). In our dataset, this may have translated into a correlation between the warmer and drier recent climate and less dynamic growth in young stands.

| Species | Effects found in this study | Convergence with the literature for some effects | Other effects found in the literature |
|---|---|---|---|
| *Picea abies* | summer temperature (+, sat.)<br>summer water availability (+, sat.) | Seynave et al. (2005), Albert and Schmidt (2010), Sharma et al. (2012), Vallet and Perot (2016), Antón-Fernández et al. (2016), Brandl et al. (2018), Caicoya and Pretzsch (2021) | Seynave et al. (2005): spring temperature (+), summer temperature (-)<br>Antón-Fernández et al. (2016): summer water availability (opt.)<br>Brandl et al. (2018): winter temperature (-)<br>Caicoya and Pretzsch (2021): GS temperature (-) |
| *Fagus sylvatica* | GS temperature (+, sat.)<br>winter water availability (-)<br>summer water availability (+) | Seynave et al. (2008), Albert and Schmidt (2010), Vallet and Perot (2016), Brandl et al. (2018) | Seynave et al. (2008): summer temperature (-), winter temperature (opt.) |
| *Pinus sylvestris* | spring temperature (+)<br>winter water availability (opt.) | Fries et al. (1998), Sharma et al. (2012), Antón-Fernández et al. (2016), González-Rodríguez and Diéguez-Aranda (2021) | Vallet and Perot (2016): July water balance (+)<br>Antón-Fernández et al. (2016): summer water availability (opt.) |
| *Quercus robur* | GS water availability (+, sat.) | Pilcher and Gray (1982)*, Stimm et al. (2021)* | Pilcher and Gray (1982)*: winter temperature (-), GS temperature (+)<br>Stimm et al. (2021)*: summer temperature (+, sat.) |
| *Quercus petraea* | spring temperature (+, sat.)<br>winter water availability (+) | Pilcher and Gray (1982)*, Vallet and Perot (2016) | Pilcher and Gray (1982)*: GS water availability (+), winter temperature (-)<br>Stimm et al. (2021)*: summer temperature (+, sat.), GS water availability (+) |

*Table 2: Comparison between the partial effects of climatic variables in our study and in the literature for the five most common tree species in Europe. '+': positive impact; '-': negative impact; 'sat.' means that the effect saturates at the higher range of the variable's distribution; 'GS': growing season (spring and summer); *: studies that did not distinguish between Quercus petraea and Quercus robur, 'opt.': optimal value. 'Water availability' refers both to precipitation and climatic water balance.*

## 4.4. Analysis of climate change during the last century on stand dominant height

Our models allow us to compare SDH dynamics under the actual recent climate (1950 to 2020) with the climate before climate change. For some species, the effects of climate change were small in the first decades of the simulations and positive thereafter. This relates to a period of relative cooling in France between 1950 and 1990, followed by a period of strong temperature increase (*cf.* Figure 1). Such temporal variations in the effects of climate change support the relevance of modeling SDH dynamics while taking into account climate variations during stand life. At the final simulation age of 70 years, the effect of climate change on SDH varied between species and between stands for a given species. In the following sections, we analyze first the interspecific and then the intraspecific variation of the site index in response to climate change, where site index Is defined as SDH at the age of 70 years.

### 4.4.1. Interspecific analysis

Our results confirm our hypothesis 2a that climate change during the last century has had different effects on different species, both in terms of sign and magnitude. The increase in the site index over the period considered for the majority of species studied is consistent with an increase in forest productivity over the last decades (Boisvenue and Running, 2006; Bontemps et al. 2009; Messaoud et al., 2022). Together with nitrogen deposition and CO2 increase, climate change is a key driver of recent changes in forest growth in Europe (Boisvenue and Running, 2006; Bontemps et al. 2009; Charru et al. 2017).

639 Interspecific differences in the effect of climate change on SDH may be related to differences
640 in species ecology, but also to interspecific differences in the pre-climate change climate
641 niche and the actual climate change experienced by the species (*cf.* Figure 1 and
642 Supplementary Material Fig. B.1 and Fig. B.2). We did not find a clear pattern linking the
643 species-specific mean effect of climate change on site index to species-specific mean initial
644 climate niche (*cf.* Supplementary Material Fig. F.1 and Fig. F.2). This suggests that species
645 ecology and experienced climate change are also key drivers of this effect. Studying another
646 growth variable and fewer species, Charru et al. (2017) found that species-specific mean
647 changes in basal area increment between 1982 and 2005 could be related to species-
648 specific mean initial climate niche, with a more positive effect for species that initially
649 experienced the coldest temperature and highest precipitation. When focusing on the same
650 species as Charru et al. (2017), our results suggest such a pattern.

651 Our results shed light on past limitations to species growth and provide insight into future
652 impacts of ongoing climate change. Over the period we considered, climate change affected
653 all species in two ways: increasing annual and summer mean temperature as well as
654 decreasing summer precipitation and / or climatic water balance (*cf.* Supplementary
655 Material Fig. B.1 and Fig. B.2). Increasing temperature favor simulated height growth, while
656 decreasing summer precipitation or climatic water balance negatively affects growth (*cf.*
657 section 4.3.). The generally positive effect of climate change on the site index we found for
658 the period 1950-2020 compared to the climate of 1891-1920 probably reflects that most of
659 the species studied were temperature-limited in France during the period 1891-1920. Our
660 finding of a strong positive effect of climate change on mountain species (*Larix decidua*,
661 *Abies alba*, and to a lesser extent *Picea abies*) is consistent with the fact that mountain
662 species are particularly temperature-limited (Charru et al., 2017). Nevertheless, the

positive effect of climate change on SDH could turn negative if temperature continue to increase and precipitation continue to decrease, due to saturation of the positive partial effect of temperature increase and the negative partial effect of precipitation (or climatic water balance ) decrease (*cf.* section 4.3.). Studies have already found observations of negative impacts of climate change on growth under water limitation (Lindner et al., 2014) or projected negative impacts on site index of future climate change Albert and Schmidt (2010). We also found such negative effects of climate change for *Pseudotsuga menziesii* and *Quercus robur*. The negative effect on *Castanea sativa* should be interpreted with caution (see 4.3).

#### 4.4.2. Intraspecific analysis

Our results confirm our hypothesis H2b that, for a given species, the impact of climate change over the last century varied among stands depending on their climate context. Intraspecific variation in the impact of climate change on site index can be related to differences in environmental conditions, management history, or plant genetics (Kremer et al., 2012). Here, we focused on the first dimension, as the French NFI does not provide data on management history or genetics. The intraspecific relationship we found between climate change effects and initial stand temperature for a large number of species reflects that, for a given species, different climatic contexts produce different growth limitations (Lindner et al., 2014; Kunstler et al., 2021; Guyennon et al., 2023). For nine species, our results suggest that climate change alleviated a temperature limitation at the cold edge of the species' distribution in France, while it had only a small positive or even negative effect on stands at the warm edge of the distribution. Such a pattern is consistent with the results of Albert and Schmidt (2010), Messaoud and Chen (2011) and Ols et al. (2020). The

686 mountain species we analyzed (*Abies alba*, *Picea abies*, *Larix decidua*) follow this pattern,
687 which is consistent with the temperature limitation they experience at high altitudes
688 (Charru et al., 2017). Finally, *Pinus halepensis* follows the same pattern, probably because it
689 is adapted to warmer climates than that of France. For the other species, the identification
690 of intraspecific patterns relating climate change effects to the reference climate is more
691 complex.

### 692 4.5. Implication for management

693 Our results raise awareness of the risk of switching from positive climate change effect on
694 SDH to negative effects due to ongoing climate change. The magnitude and timing of this
695 switch for a given stand will depend on the species, the current climatic context and the
696 climate change that the stand will experience. Our results may help forest managers to
697 identify which species to favor when managing a pure even-aged stand. Furthermore, our
698 models could be used to project SDH dynamics under future climate scenarios, although
699 caution should be taken when running simulations outside the calibration range of
700 empirical models. Thus, it may be useful to integrate our work into models used to inform
701 management strategy.

702 Our results also suggest that climate change may alter the relative competitiveness of
703 species for light in mixed stands, due to interspecific differences in the effect of climate
704 change on SDH dynamics. This may lead to changes in forest composition if climate change
705 penalizes the height growth of some shade-intolerant species more than the height growth
706 of shade-tolerant species (Bontemps et al., 2012; Messaoud et al., 2022). Taking this effect
707 into account is important for the management of mixed stands. This is even more true in a

context where forest managers are encouraged to diversify species to adapt forests to climate change.

## 5. Conclusion

For 20 European species, we developed stand dominant height dynamics models taking into account annual climate, based on data from more than 17,000 forest stands surveyed by the French National Forest Inventory and a 150-years climate database.

We found that climate change over the past century had contrasting effects between and within species. For the majority of species studied, most stands have benefited from climate change, as shown by comparing the average climate of 1891-1920 with the actual recent climate of 1950-2020. For some species, however, we found that a significant percentage of stands were already experiencing negative impacts. The relationship between temperature and within-species differences in climate change effects suggests that climatic context may drive differences in response to climate change for a given species.

These results suggest that future forest response to continued climate change will vary by species, initial stand climate context, and stand climate trends. They also suggest that continued increases in temperature and decreases in summer precipitation may lead to more negative trends than observed in the past. Consideration of these different aspects is critical to inform management to adapt forests to future climate change.

## Additional files

- Supplementary Material (provided in a separate file) contains additional information regarding some points mentioned in the main text

- R code to prepare data, calibrate models and analyze results as well as model parameters are available at https://github.com/matthieucombaud/paper_dominant-height-20-species

## Data Availability Statement

- French NFI data that support the findings of this study are openly available at IGN – Inventaire forestier national français, Données brutes, Campagnes annuelles 2005 et suivantes, https://inventaire-forestier.ign.fr/dataIFN/. NFI's stands exact altitudes were obtained from IGN – Inventaire forestier national (contact: https://www.ign.fr)

- FYRE climate data that support the findings of this study are openly available on Zenodo, for precipitation (Devers, Alexandre, Vidal, Jean-Philippe, Lauvernet, Claire, & Vannier, Olivier. (2020a). *FYRE Climate: Precipitation* [Data set]. Zenodo. https://doi.org/10.5281/ZENODO.4005573) and for temperature (Devers, Alexandre, Vidal, Jean-Philippe, Lauvernet, Claire, & Vannier, Olivier. (2020b). *FYRE Climate: Temperature* [Data set]. https://doi.org/10.5281/zenodo.4006472)

- Safran climate data were obtained from Meteo France through the SICLIMA platform (https://agroclim.inrae.fr/siclima/). Meteo France can be contacted through the webpage https://donneespubliques.meteofrance.fr/

## Acknowledgement

This work was supported by the metaprogramme "Agriculture and forestry in the face of climate change: adaptation and mitigation" (CLIMAE) of the French National Research Institute for Agriculture, Food and Environment (INRAE) and the French National Forest Office (ONF). The authors wish to thank the French NFI for providing the stand data, Météo-France for providing the SAFRAN data, Jean-Claude Gégout for providing data on bioindication, Alexandre Devers and Jean-Philippe Vidal for exchanges on climate data, Christian Piedallu for exchanges about bioindicated values, Björn Reineking and Carine Babusiaux for helping on the optimization algorithm, Cécile Robin for sharing her view on *Castanea sativa*, Thomas Pérot, Anne Baranger and Nathéo Beauchamp for re-reading some parts of the manuscript, and Mathieu Jonard, Xavier Morin, Jordan Bello and François Morneau for discussing the general idea of the paper. The authors also want to thanks the participants of the 2023 FOREM seminar for their constructive inputs.

## References

Aguirre, Ana, Daniel Moreno-Fernández, Iciar Alberdi, Laura Hernández, Patricia Adame, Isabel Cañellas, and Fernando Montes. 2022. "Mapping Forest Site Quality at National Level." *Forest Ecology and Management* 508 (March): 120043. https://doi.org/10.1016/j.foreco.2022.120043.

Albert, M., and M. Schmidt. 2010. "Climate-Sensitive Modelling of Site-Productivity Relationships for Norway Spruce (Picea Abies (L.) Karst.) and Common Beech (Fagus Sylvatica L.)." *Forest Ecology and Management*, Adaptation of Forests and Forest Management to Changing Climate, 259 (4): 739–49. https://doi.org/10.1016/j.foreco.2009.04.039.

Álvarez-Álvarez, Pedro, Elías Afif Khouri, Asunción Cámara-Obregón, Fernando Castedo-Dorado, and Marcos Barrio-Anta. 2011. "Effects of Foliar Nutrients and Environmental

773 Factors on Site Productivity in Pinus Pinaster Ait. Stands in Asturias (NW Spain)." *Annals of*
774 *Forest Science* 68 (3): 497–509. https://doi.org/10.1007/s13595-011-0047-5.

775 Anderson-Teixeira, Kristina J., Valentine Herrmann, Christine R. Rollinson, Bianca Gonzalez,
776 Erika B. Gonzalez-Akre, Neil Pederson, M. Ross Alexander, et al. 2022. "Joint Effects of
777 Climate, Tree Size, and Year on Annual Tree Growth Derived from Tree-Ring Records of Ten
778 Globally Distributed Forests." *Global Change Biology* 28 (1): 245–66.
779 https://doi.org/10.1111/gcb.15934.

780 Antón-Fernández, Clara, Blas Mola-Yudego, Lise Dalsgaard, and Rasmus Astrup. 2016.
781 "Climate-Sensitive Site Index Models for Norway." *Canadian Journal of Forest Research* 46
782 (6). https://cdnsciencepub.com/doi/full/10.1139/cjfr-2015-0155.

783 Asshoff, Roman, Gerhard Zotz, and Christian Körner. 2006. "Growth and Phenology of
784 Mature Temperate Forest Trees in Elevated CO2." *Global Change Biology* 12 (5): 848–61.
785 https://doi.org/10.1111/j.1365-2486.2006.01133.x.

786 Assmann, Ernst, and P. W. Davis. 1970. *Principles of Forest Yield Study*. Pergamon.

787 Boisvenue, Céline, and Steven W. Running. 2006. "Impacts of Climate Change on Natural
788 Forest Productivity – Evidence since the Middle of the 20th Century." *Global Change Biology*
789 12 (5): 862–82. https://doi.org/10.1111/j.1365-2486.2006.01134.x.

790 Bontemps, Jean-Daniel, and Olivier Bouriaud. 2014. "Predictive Approaches to Forest Site
791 Productivity: Recent Trends, Challenges and Future Perspectives." *Forestry: An*
792 *International Journal of Forest Research* 87 (1): 109–28.
793 https://doi.org/10.1093/forestry/cpt034.

794 Bontemps, Jean-Daniel, Jean-Christophe Hervé, and Jean-François Dhôte. 2009. "Long-Term
795 Changes in Forest Productivity: A Consistent Assessment in Even-Aged Stands." *Forest*
796 *Science* 55 (6): 549–64. https://doi.org/10.1093/forestscience/55.6.549.

797 Bontemps, Jean-Daniel, Jean-Christophe Herve, Pierre Duplat, and Jean-François Dhôte.
798 2012. "Shifts in the Height-Related Competitiveness of Tree Species Following Recent
799 Climate Warming and Implications for Tree Community Composition: The Case of Common
800 Beech and Sessile Oak as Predominant Broadleaved Species in Europe." *Oikos* 121 (8):
801 1287–99. https://doi.org/10.1111/j.1600-0706.2011.20080.x.

802 Bontemps, Jean-Daniel, Jean-Christophe Hervé, Jean-Michel Leban, and Jean-François Dhôte.
803 2011. "Nitrogen Footprint in a Long-Term Observation of Forest Growth over the Twentieth
804 Century." *Trees* 25 (2): 237–51. https://doi.org/10.1007/s00468-010-0501-2.

805 Brandl, S., T. Mette, W. Falk, Patrick Vallet, T. Rötzer, and H. Pretzsch. 2018. "Static Site
806 Indices from Different National Forest Inventories: Harmonization and Prediction from Site
807 Conditions." *Annals of Forest Science* 75 (2). https://doi.org/10.1007/s13595-018-0737-3.

808 Bravo-Oviedo, A., M. Tomé, F. Bravo, G. Montero, and M. Del Río. 2008. "Dominant Height
809 Growth Equations Including Site Attributes in the Generalized Algebraic Difference
810 Approach." *Canadian Journal of Forest Research* 38 (9): 2348–58.
811 https://doi.org/10.1139/X08-077.

812 Caicoya, A.T., and H. Pretzsch. 2021. “Stand Density Biases the Estimation of the Site Index
813 Especially on Dry Sites.” *Canadian Journal of Forest Research* 51 (7): 1050–64.
814 https://doi.org/10.1139/cjfr-2020-0389.

815 Caillouet, Laurie, Jean-Philippe Vidal, Eric Sauquet, Benjamin Graff, and Jean-Michel
816 Soubeyroux. 2019. “SCOPE Climate: A 142-Year Daily High-Resolution Ensemble
817 Meteorological Reconstruction Dataset over France.” *Earth System Science Data* 11 (1):
818 241–60. https://doi.org/10.5194/essd-11-241-2019.

819 Charru, Marie, Ingrid Seynave, Jean-Christophe Hervé, Romain Bertrand, and Jean-Daniel
820 Bontemps. 2017. “Recent Growth Changes in Western European Forests Are Driven by
821 Climate Warming and Structured across Tree Species Climatic Habitats.” *Annals of Forest*
822 *Science* 74 (2): 33. https://doi.org/10.1007/s13595-017-0626-1.

823 Devers, Alexandre, Jean-Philippe Vidal, Claire Lauvernet, Benjamin Graff, and Olivier
824 Vannier. 2020. “A Framework for High-Resolution Meteorological Surface Reanalysis
825 through Offline Data Assimilation in an Ensemble of Downscaled Reconstructions.”
826 *Quarterly Journal of the Royal Meteorological Society* 146 (726): 153–73.
827 https://doi.org/10.1002/qj.3663.

828 Devers, Alexandre, Jean-Philippe Vidal, Claire Lauvernet, and Olivier Vannier. 2020a. “FYRE
829 Climate: Precipitation.” Zenodo. https://doi.org/10.5281/zenodo.4005573.

830 ———. 2020b. “FYRE Climate: Temperature.” Zenodo.
831 https://doi.org/10.5281/zenodo.4006472.

832 ———. 2021. “FYRE Climate: A High-Resolution Reanalysis of Daily Precipitation and
833 Temperature in France from 1871 to 2012.” *Climate of the Past* 17 (5): 1857–79.
834 https://doi.org/10.5194/cp-17-1857-2021.

835 Fries, Anders, Seppo Ruotsalainen, and Dag Lindgren. 1998. “Effects of Temperature on the
836 Site Productivity of Pinus Sylvestris and Lodgepole Pine in Finland and Sweden.”
837 *Scandinavian Journal of Forest Research* 13 (1–4): 128–40.
838 https://doi.org/10.1080/02827589809382969.

839 Gégout, Jean-Claude, Christophe Coudun, Gilles Bailly, and Bernard Jabiol. 2005. “EcoPlant:
840 A Forest Site Database Linking Floristic Data with Soil and Climate Variables.” *Journal of*
841 *Vegetation Science* 16 (2): 257–60. https://doi.org/10.1111/j.1654-1103.2005.tb02363.x.

842 González-Rodríguez, M.Á., and U. Diéguez-Aranda. 2020. “Exploring the Use of Learning
843 Techniques for Relating the Site Index of Radiata Pine Stands with Climate, Soil and
844 Physiography.” *Forest Ecology and Management* 458.
845 https://doi.org/10.1016/j.foreco.2019.117803.

846 ———. 2021. “Rule-Based vs Parametric Approaches for Developing Climate-Sensitive Site
847 Index Models: A Case Study for Scots Pine Stands in Northwestern Spain.” *Annals of Forest*
848 *Science* 78 (1). https://doi.org/10.1007/s13595-021-01047-2.

849 Guyennon, Arnaud, Björn Reineking, Roberto Salguero-Gomez, Jonas Dahlgren, Aleksi
850 Lehtonen, Sophia Ratcliffe, Paloma Ruiz-Benito, Miguel A. Zavala, and Georges Kunstler.

2023. “Beyond Mean Fitness: Demographic Stochasticity and Resilience Matter at Tree Species Climatic Edges.” *Global Ecology and Biogeography* 32 (4): 573–85. https://doi.org/10.1111/geb.13640.

Harris, Ian, Timothy J. Osborn, Phil Jones, and David Lister. 2020. “Version 4 of the CRU TS Monthly High-Resolution Gridded Multivariate Climate Dataset.” *Scientific Data* 7 (1): 109. https://doi.org/10.1038/s41597-020-0453-3.

IGN. 2022. “Données Brutes de l’inventaire Forestier Mises En Ligne Sur DataIFN - Version 2.0.” https://inventaire-forestier.ign.fr/dataIFN/.

Kremer, Antoine, Ophélie Ronce, Juan J. Robledo-Arnuncio, Frédéric Guillaume, Gil Bohrer, Ran Nathan, Jon R. Bridle, et al. 2012. “Long-Distance Gene Flow and Adaptation of Forest Trees to Rapid Climate Change.” *Ecology Letters* 15 (4): 378–92. https://doi.org/10.1111/j.1461-0248.2012.01746.x.

Kristensen, Kasper, Anders Nielsen, Casper W. Berg, Hans Skaug, and Brad Bell. 2016. “TMB: Automatic Differentiation and Laplace Approximation.” *Journal of Statistical Software* 70 (5). https://doi.org/10.18637/jss.v070.i05.

Kunstler, Georges, Arnaud Guyennon, Sophia Ratcliffe, Nadja Rüger, Paloma Ruiz-Benito, Dylan Z. Childs, Jonas Dahlgren, et al. 2021. “Demographic Performance of European Tree Species at Their Hot and Cold Climatic Edges.” *Journal of Ecology* 109 (2): 1041–54. https://doi.org/10.1111/1365-2745.13533.

Lebourgeois, F., and C. Piedallu. 2005. “Appréhender le niveau de sécheresse dans le cadre des études stationnelles et de la gestion forestière? Notion d’indices bioclimatiques, méthode d’estimation de l’évapotranspiration potentielle.” *Revue Forestière Française*.

Lindner, Marcus, Joanne B. Fitzgerald, Niklaus E. Zimmermann, Christopher Reyer, Sylvain Delzon, Ernst van der Maaten, Mart-Jan Schelhaas, et al. 2014. “Climate Change and European Forests: What Do We Know, What Are the Uncertainties, and What Are the Implications for Forest Management?” *Journal of Environmental Management* 146 (December): 69–83. https://doi.org/10.1016/j.jenvman.2014.07.030.

Lindner, Marcus, Michael Maroschek, Sigrid Netherer, Antoine Kremer, Anna Barbati, Jordi Garcia-Gonzalo, Rupert Seidl, et al. 2010. “Climate Change Impacts, Adaptive Capacity, and Vulnerability of European Forest Ecosystems.” *Forest Ecology and Management*, Adaptation of Forests and Forest Management to Changing Climate, 259 (4): 698–709. https://doi.org/10.1016/j.foreco.2009.09.023.

Mahnken, Mats, Maxime Cailleret, Alessio Collalti, Carlo Trotta, Corrado Biondo, Ettore D’Andrea, Daniela Dalmonech, et al. 2022. “Accuracy, Realism and General Applicability of European Forest Models.” *Global Change Biology* 28 (23): 6921–43. https://doi.org/10.1111/gcb.16384.

Maurel, Marion, Cécile Robin, Xavier Capdevielle, Denis Loustau, and Marie-Laure Desprez-Loustau. 2001. “Effects of Variable Root Damage Causedby *Phytophthora Cinnamomi* on Water Relationsof Chestnut Saplings.” *Annals of Forest Science* 58 (6): 639–51. https://doi.org/10.1051/forest:2001151.

McDowell, Nate G., Craig D. Allen, Kristina Anderson-Teixeira, Brian H. Aukema, Ben Bond-Lamberty, Louise Chini, James S. Clark, et al. 2020. “Pervasive Shifts in Forest Dynamics in a Changing World.” *Science* 368 (6494): eaaz9463. https://doi.org/10.1126/science.aaz9463.

Messaoud, Y., and H.Y.H. Chen. 2011. “The Influence of Recent Climate Change on Tree Height Growth Differs with Species and Spatial Environment.” *PLoS ONE* 6 (2). https://doi.org/10.1371/journal.pone.0014691.

Messaoud, Yassine, Anya Reid, Nadezhda M. Tchebakova, Jack A. Goldman, and Annika Hofgaard. 2022. “The Historical Complexity of Tree Height Growth Dynamic Associated with Climate Change in Western North America.” *Forests* 13 (5): 738. https://doi.org/10.3390/f13050738.

Mina, Marco, Markus O. Huber, David I. Forrester, Esther Thürig, and Brigitte Rohner. 2018. “Multiple Factors Modulate Tree Growth Complementarity in Central European Mixed Forests.” *Journal of Ecology* 106 (3): 1106–19. https://doi.org/10.1111/1365-2745.12846.

O’Brien, Robert M. 2007. “A Caution Regarding Rules of Thumb for Variance Inflation Factors.” *Quality & Quantity* 41 (5): 673–90. https://doi.org/10.1007/s11135-006-9018-6.

Ols, Clémentine, Jean-Christophe Hervé, and Jean-Daniel Bontemps. 2020. “Recent Growth Trends of Conifers across Western Europe Are Controlled by Thermal and Water Constraints and Favored by Forest Heterogeneity.” *Science of The Total Environment* 742 (November): 140453. https://doi.org/10.1016/j.scitotenv.2020.140453.

Pau, Mathilde, Sylvie Gauthier, Raphaël D. Chavardès, Martin P Girardin, William Marchand, and Yves Bergeron. 2022. “Site Index as a Predictor of the Effect of Climate Warming on Boreal Tree Growth.” *Global Change Biology* 28 (5): 1903–18. https://doi.org/10.1111/gcb.16030.

Piedallu, Christian, and J.C. Gégout. 2007. “Multiscale Computation of Solar Radiation for Predictive Vegetation Modelling.” *Annals of Forest Science* 64 (8): 899 909. https://doi.org/10.1051/forest:2007072.

Piedallu, Christian, Noémie Pousse, Ary Bruand, Lucie Dietz, and Julien Fiquepron. 2018. “Quelles Fonctions de Pédotransfert Le Forestier Doit-Il Utiliser ?” *Forêt-Entreprise*, no. 242.

Pilcher, Jonathan, and B. Gray. 1982. “The Relationships between Oak Tree Growth and Climate in Britain.” *The Journal of Ecology* 70 (March): 297. https://doi.org/10.2307/2259880.

R Core Team. 2022. “R: A Language and Environment for Statistical Computing.” Vienne, Austria: R Foundation for Statistical Computing. https://www.R-project.org/.

Scolforo, H.F., J.P. McTague, H. Burkhart, J. Roise, C.A. Alvares, and J.L. Stape. 2020. “Site Index Estimation for Clonal Eucalypt Plantations in Brazil: A Modeling Approach Refined by Environmental Variables.” *Forest Ecology and Management* 466. https://doi.org/10.1016/j.foreco.2020.118079.

Seynave, Ingrid, J.-C. Gégout, J.-C. Hervé, J.-F. Dhôte, J. Drapier, E. Bruno, and G. Dumé. 2005. “Picea Abies Site Index Prediction by Environmental Factors and Understorey Vegetation: A

Two-Scale Approach Based on Survey Databases." *Canadian Journal of Forest Research* 35 (7): 1669–78. https://doi.org/10.1139/x05-088.

Seynave, Ingrid, Jean-Claude Gégout, Jean-Christophe Hervé, and Jean-François Dhôte. 2008. "Is the Spatial Distribution of European Beech (Fagus Sylvatica L.) Limited by Its Potential Height Growth?" *Journal of Biogeography* 35 (10): 1851–62. https://doi.org/10.1111/j.1365-2699.2008.01930.x.

Sharma, M., N. Subedi, M. Ter-Mikaelian, and J. Parton. 2015. "Modeling Climatic Effects on Stand Height/Site Index of Plantation-Grown Jack Pine and Black Spruce Trees." *Forest Science* 61 (1): 25–34. https://doi.org/10.5849/forsci.13-190.

Sharma, R.P., A. Brunner, and T. Eid. 2012. "Site Index Prediction from Site and Climate Variables for Norway Spruce and Scots Pine in Norway." *Scandinavian Journal of Forest Research* 27 (7): 619–36. https://doi.org/10.1080/02827581.2012.685749.

Skovsgaard, J. P., and J. K. Vanclay. 2008. "Forest Site Productivity: A Review of the Evolution of Dendrometric Concepts for Even-Aged Stands." *Forestry: An International Journal of Forest Research* 81 (1): 13–31. https://doi.org/10.1093/forestry/cpm041.

Socha, J., L. Tyminska-Czabanska, E. Grabska, and S. Orzeł. 2020. "Site Index Models for Main Forest-Forming Tree Species in Poland." *Forests* 11 (3). https://doi.org/10.3390/f11030301.

Socha, Jarosław, Svein Solberg, Luiza Tymińska-Czabańska, Piotr Tompalski, and Patrick Vallet. 2021. "Height Growth Rate of Scots Pine in Central Europe Increased by 29% between 1900 and 2000 Due to Changes in Site Productivity." *Forest Ecology and Management* 490 (June): 119102. https://doi.org/10.1016/j.foreco.2021.119102.

Stimm, Kilian, Michael Heym, Enno Uhl, Stefan Tretter, and Hans Pretzsch. 2021. "Height Growth-Related Competitiveness of Oak (Quercus Petraea (Matt.) Liebl. and Quercus Robur L.) under Climate Change in Central Europe. Is Silvicultural Assistance Still Required in Mixed-Species Stands?" *Forest Ecology and Management* 482 (February): 118780. https://doi.org/10.1016/j.foreco.2020.118780.

Tomé, José, Margarida Tomé, Susana Barreiro, and Joana Amaral Paulo. 2006. "Age-Independent Difference Equations for Modelling Tree and Stand Growth." *Canadian Journal of Forest Research* 36 (7): 1621–30. https://doi.org/10.1139/x06-065.

Valentine, Harry T. 1997. "Height Growth, Site Index, and Carbon Metabolism." https://doi.org/10.14214/sf.a8524.

Vallet, Patrick, and Thomas Perot. 2016. "Tree Diversity Effect on Dominant Height in Temperate Forest." *Forest Ecology and Management* 381: 106–14. https://doi.org/10.1016/j.foreco.2016.09.024.

Vidal, Jean-Philippe, Eric Martin, Laurent Franchistéguy, Martine Baillon, and Jean-Michel Soubeyroux. 2010. "A 50-Year High-Resolution Atmospheric Reanalysis over France with the Safran System." *International Journal of Climatology* 30 (11): 1627–44. https://doi.org/10.1002/joc.2003.

969 Zeide, Boris. 1993. “Analysis of Growth Equations.” *Forest Science* 39 (3): 594–616.
970 https://doi.org/10.1093/forestscience/39.3.594.

971

972